Rheol Acta 38: 145–159 (1999)

ORIGINAL CONTRIBUTION

C. Bower
C. Gallegos
M.R. Mackley
J.M. Madiedo

The rheological and microstructural characterisation of the non-linear flow behaviour of concentrated oil-in-water emulsions

Received: 10 November 1998
Accepted: 24 November 1998

C. Bower · M.R. Mackley (✉)
Department of Chemical Engineering
University of Cambridge
New Museums Site, Pembroke Street
Cambridge, CB2 3RA, UK
http://www.cheng.cam.ac.uk

C. Gallegos · J.M. Madiedo
Departamento de Ingeniera Química
Universidad de Huelva
21819 Palos de la Frontera, Huelva, SPAIN
http://reologia.us.es

Abstract This paper reports experimental observations on the rheology and microstructure of concentrated oil-in-water emulsions stabilised by macromolecular and low-molecular-weight emulsifiers. From the four different samples that were tested, certain general trends were identified and the measured linear viscoelastic and non-linear viscoelastic properties were compared using a phenomenological factored integral constitutive equation with a continuous relaxation spectrum. The self-consistency of the model was quite good in two cases (vegetable protein and polyoxyethylene glycol non-ionic surfactant emulsifiers) with the general exception of low steady shear rate data where the model overpredicted experimental stress measurements. It is shown that the fitting of the experimental data is sensitive to a wide range of inter-relating factors. In addition, optical observations of the sheared materials consistently showed low shear rate surface slip and this observation was correlated with the rheology miss match. For some systems the optical microstructure studies reveal a range of behaviour for the emulsions dependent on emulsifier composition. Wall slip, microdomain movement, chaining and changes in droplet size distribution were all observed under different conditions and in some cases it has been possible to correlate these microstructure observations with the sample rheology.

Key words Oil-in-water emulsions – Microstructure – Rheology slip

Introduction

Concentrated oil-in-water emulsions show a very complex rheological behaviour (Barnes 1994; Tadros 1993). In general, the material shear thins in steady shear (Barnes 1994), showing a zero-shear-rate-limiting viscosity at shear rates of order 10^{-4} s^{-1} or lower. At shear rates higher than the critical one for the onset of the shear-thinning region, the viscosity is approximately proportional to $\dot{\gamma}^{-1}$. This behaviour has been mainly associated to droplet deflocculation, although other mechanisms may develop as the shear rate increases. The same behaviour is also shown by flocculated suspensions (Barnes 1995). Several well-known steady-state flow models (Ostwald-de Waele, Cross, Carreau) have been used to fit this viscous response (Pal 1992; Pal and Rhodes 1989; Partal et al. 1994).

In oscillatory shear, the evolution of the linear viscoelasticity functions in a frequency range between 10^{-2} and 10^{2} rad/s, for commercial mayonnaise, is characterised by the appearance of a minimum in the loss modulus at intermediate frequencies and a "plateau region" in the storage modulus (slope values of around 0.1). In addition, the frequency dependence of both moduli is clearly dependent on the emulsion concentration, processing conditions and nature of the emulsifier used (Franco et al. 1995, 1997; Tadros 1993). Thus, a more general picture of the oscillatory response of

emulsions stabilised by macromolecular and/or low-molecular-weight emulsifiers presents three characteristic regions: a pseudo-terminal region at low frequencies, an intermediate "plateau" region, and the beginning of the transition region at high frequencies. These linear viscoelastic properties can be matched, for example, to a Generalised Maxwell Mode, with discrete or continuous spectrum (Guerrero et al. 1996). Franco et al. (1995) have used the BSW-CW model to successfully describe the above-mentioned regions in the linear relaxation spectra of emulsions stabilised by a mixture of macromolecular and low-molecular-weight emulsifiers. Madiedo and Gallegos (1997) have used a different empirical model that describes those regions in the relaxation spectra of oil-in-water emulsions stabilised by a mixture of two low-molecular-weight surfactants with different hydrophilic-lipophilic balances.

The combined matching of the linear viscoelastic response, the non-linear viscoelastic response and steady-state flow behaviour of oil-in-water emulsions is a more challenging problem. Up to now a limited number of attempts have been made and in each case these have involved using an integral form Wagner equation where time and strain is separate. Mackley et al. (1994) used this model and a discrete relaxation spectrum to predict the steady-state flow behaviour of a variety of materials, although this application to commercial mayonnaise was without great success. Other authors (Gallegos et al. 1992a; Gallegos and Franco 1995) applied a modified Wagner model, where the Wagner damping function was changed for the Soskey-Winter one (Soskey and Winter 1984), to fit the transient flow behaviour of different commercial and model food emulsions, achieving relatively good results for low shear rates, although absolute values were not well predicted. No precise explanations were made for the reasons of the generalised failure of the above-mentioned model, although some answers can be extracted from the conclusions of the present work.

It is reasonable to assume that the flow behaviour of concentrated oil-in-water emulsions must correlate with the evolution of the structure with shear and this paper is concerned with elucidating the primary factors that control the flow behaviour of a range of oil-in-water emulsions, stabilised using macromolecular or low-molecular-weight emulsifiers. In order to achieve this aim, both experimental and modelling aspects have been considered. The applicability of a phenomenological model able to describe both the linear viscoelastic and steady-state flow behaviour of the emulsions has been tested. A Wager-type factored constitutive equation has been chosen on the basis that it has previously been shown to successfully bridge the gap between small strain viscoelasticity and steady-state shear for a number of structured fluids (Mackley et al. 1994). In addition, an attempt to correlate microstructural observations and flow behaviour of the deformed emulsions using a specially designed optical shear cell (Bower et al. 1997) has been addressed.

Rheological modelling

The Wagner model derives from the more general KBKZ model (Larson 1988). It was initially derived as an equation that empirically described polymer melt behaviour; more recently, Wagner has attempted to relate the model to molecular parameters (Wagner and Schaeffer 1993). Considering only the shear stress component of the stress tensor and time-strain separability, a form of the KBKZ equation is:

$$\tau(t) = -\int_{-\infty}^{t} \frac{\mathrm{d}G(t-t')}{\mathrm{d}t'} h(\gamma)\gamma(t,t')\mathrm{d}t \tag{1}$$

where $G(t-t')$ is the linear relaxation modulus and $h(\gamma)$ is a damping function. Following Wagner (1976)

$$h(\gamma)\mathrm{e}^{-k|\gamma(t,t')|} \tag{2}$$

where the damping factor, k, is an empirical parameter which quantifies the level of non-linearity in the material. This function can be calculated from the ratio between the non-linear relaxation modulus, $G(\gamma,t-t')$, and the linear relaxation modulus, $G(t-t')$:

$$h(\gamma) = \frac{G(\gamma, t-t')}{G(t-t')} \tag{3}$$

In this integral equation, the relaxation modulus may be described in the usual way in terms of a discrete set of Maxwell elements, or as a continuous spectrum where the relaxation modulus can be related to the continuous relaxation spectrum by the equation:

$$G(t-t') = \int_{-\infty}^{\infty} H(\lambda)\mathrm{e}^{-(t-t')/\lambda}\mathrm{d}\ \mathrm{l}n\lambda \tag{4}$$

Substituting this into Eq. (1), the Wagner model gives:

$$\tau(t) = -\int_{-\infty}^{t}\int_{-\infty}^{\infty} H(\lambda)\mathrm{e}^{-(t-t')/\lambda}\mathrm{e}^{-k|\gamma(t,t')|}\gamma(t,t')\mathrm{d}\ \mathrm{l}n\lambda\ \mathrm{d}t' \tag{5}$$

and the apparent viscosity can be calculated from the following integral equation:

$$\eta(\gamma) = \int_{-\infty}^{\infty} \frac{\lambda H(\lambda)}{(1+k\lambda\gamma)^2}\mathrm{d}\ \mathrm{l}n\lambda \tag{6}$$

In order to obtain the continuous spectrum for each emulsion tested, the Tikhonov regularization method was used (Madiedo et al. 1996; Madiedo and Gallegos 1997). There are now a wide range of numerical techniques available for determining relaxation spectra, the method chosen here has been developed by some of the authors (Madiedo and Gallegos 1997).

Experimental procedures

Sample preparation

Four emulsion systems were chosen and three of the emulsions were made using sunflower oil (Hijos de Ybarra, Seville, Spain) and water. The other emulsion tested was a commercial mayonnaise (Hellmanns, UK). The vegetable protein-stabilised emulsion was made from 65% wt sunflower oil, 30% wt water and 5% wt, dried pea protein (System Bio-industries, Barcelona, Spain). The pea protein powder was dispersed in water to form a very fine suspension, and the oil was then slowly added to the suspension whilst stirring using a turbine mixer (T25basic from IKA, Germany). Two low-molecular-weight non-ionic emulsifiers were also used: a polyoxyethylene glycol nonylphenylether (PEG) and a sucrose stearate (SS). PEG-stabilised emulsion was made in a similar way to the pea protein-stabilised emulsion. Thus, 3% wt PEG emulsifier (Triton N101, Sigma, St. Louis, USA) was mixed with 27% wt water to form a homogeneous solution, at room temperature. Then, 70% wt sunflower oil was slowly added whilst under agitation to form a stable emulsion. The sucrose ester-stabilised emulsion was made under slightly different conditions in that 5% wt sucrose ester powder (S-1570 from Mitsubishi Kasei Food Corporation, Japan) was initially mixed with 25% wt water at 50 °C in order to form a surfactant solution. The 70% wt sunflower oil was then progressively added at that temperature whilst under agitation. After the emulsion had been formed it was allowed to cool to room temperature before any tests were carried out. In all cases the emulsions were stable for periods in excess of 1 month.

Rhelogical characterisation

Rheological characterisation of the emulsions was performed using a RDSII dynamic spectrometer (Rheometric Scientific), a controlled-strain device that for the purpose of the experiments performed here, was fitted with a parallel plate test tool (50 mm diameter). A controlled strain or steady shear rate was applied to the test sample and the resultant torque and normal force measured with a force transducer. Rheological characterisation was done using a series of tests, described in more detail by Mackley et al. (1994).

Firstly the extent of the linear behaviour was determined by performing a strain sweep to measure dynamic moduli at increasing strains. Secondly a dynamic frequency sweep (10^{-2} to 10^{2} rad/s) was carried out at an applied strain within the linear region, in order to measure dynamic moduli at variable frequencies. The dynamic moduli from the frequency sweep data could then be used to determine a spectrum of relaxation times for each material, either discrete or continuous. Next a series of step strain experiments was performed, in which the sample was subjected to a precisely controlled step strain and the resultant torque measured over the time taken for relaxation. A step strain within the linear region was carried out first, followed by a series of increasing strains in the non-linear region. The linear and non-linear step strain data could then be used to calculate the Wagner damping factor from Eq. (3). Finally the steady shear response of the material was measured by subjecting the sample to increasing steady shear rates (0.1–300 s^{-1}). Using the damping factor and Eqs. (5) and (6), the model prediction of the steady shear behaviour could be then compared with the experimental data. All the rheological measurements were carried out at 20 °C.

Microstructure observations

In addition to the rheological characterisation, experimental observations of the effects of shear rate on the emulsion microstructure were also performed. To this end a custom built optical shearing cell was used, developed in Cambridge and built by Linkam Scientific Instruments, Surrey (see for example Bower et al. 1997). The sample is placed between two circular quartz discs, and the bottom disc rotated by a stepper motor to allow application of a controlled shear rate. A second stepper motor allows the separation of the discs to be varied so that the sample gap could be adjusted from 2500 μm down to 10 μm. Changing the waveform on the input of the stepper motor allowed the shear applied to the sample to be either continuous, step or oscillatory.

With this equipment it was therefore possible to generate shear conditions identical to those on the RDSII. Temperature control was achieved using two silver-block heating elements above and below the quartz discs to allow precision temperature adjustment between 20 °C and 350 °C, although experiments reported in this paper were performed at 20 °C. Full control of the shear cell was facilitated by a software interface running on a personal computer. Figure 1 shows the top and bottom plates of the shear cell in the assembled and dis-assembled state. The optical stage was mounted on a standard Olympus optical microscope with a JVC CCD camera fitter so that experiments could be recorded onto S-VHS video tape. Feeding the signal from the CCD into a frame grabber board also allowed capture of digital images facilitating measurements of droplet size, elongation and orientation with standard image analysis software.

Results

Commercial mayonnaise

The rheological data for the commercially produced oil-in-water emulsion are presented in Fig. 2. The experimental data obtained are typical of all the oil-in-water emulsion studied in this paper. Starting with the strain sweep of Fig 2a, it is seen that the material response is linear over a very limited region of small strain, less than 1%. Figure 2b shows data for a frequency sweep performed at a strain of 0.4% fitted with a continuous spectrum of relaxation times. For the continuous spectrum fit, a time domain equivalent to the experimental frequency domain was chosen. For the material, the elastic modulus G′ is greater than the viscous modulus G″ over the entire range of applied strain or frequency, indicating the predominantly elastic behaviour of the material at these small test strains. However, the slope of the power-law frequency dependence of G′ is higher and the minimum in G″ less pronounced than for other mayonnaise-like products previously studied (Gallegos et al. 1992b). Figure-2c shows the continuous spectrum of relaxation times for the commercial mayonnaise, and it indicates a predominant "plateau" behaviour in the time domain tested, with a gradual decrease in the stiffness constant with increasing relaxation times. The results of step strain experiments are show in Fig. 2d. The non-linear behaviour of the material is apparent from the figure, where an increase in the applied strain from 1% to 50% results in a marked decrease in the relaxation modulus. The step strain data of Fig. 2d can be used to determine the Wagner damping factor to characterise the degree of

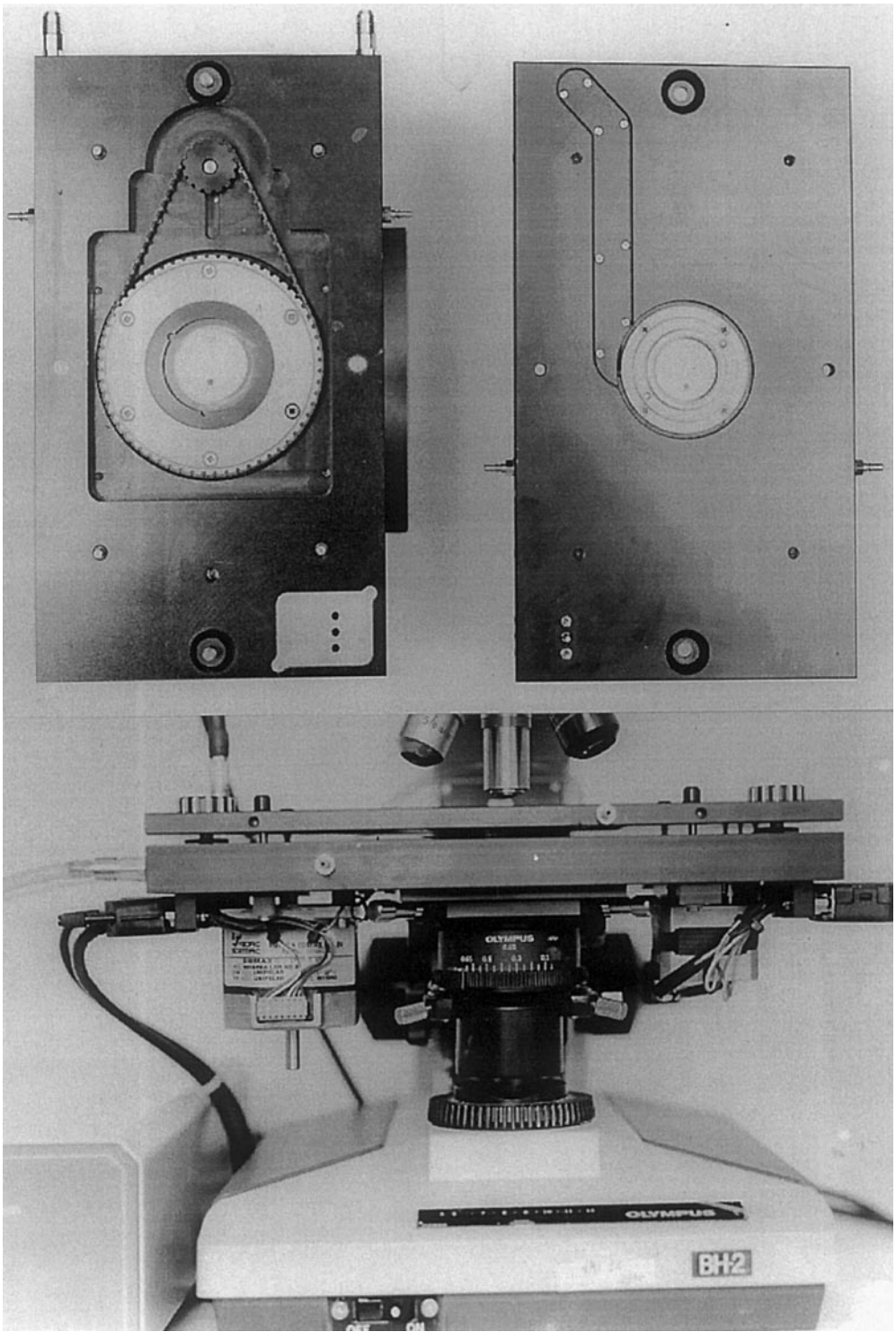

Fig. 1 Photographs of Cambridge/Linkam shear cell, showing top and bottom plate together with assembly on microscope

non-linearity. A damping factor of 0.75 has been estimated. The damping factor can then be used to make a prediction of the response of the material when subjected to a steady shear rate. Figure 2e shows the steady shear data for the commercial mayonnaise studied. The data are fitted with a prediction from the integral constitutive equation with Wagner damping factor, using a continuous spectrum of relaxation times.

However, the fit is not particularly good at either low on high shear rates. The overestimation of the apparent viscosity at low shear rates is thought to be due to sample slipping between the rheometer plates, as reported previously for other emulsions (Barnes 1995; Franco et al. 1998).

The optical microstructures observed for the commercial mayonnaise studied are shown in Fig. 3, for a series of increasing shear rates. The optical observation during shearing has proved to be a useful addition to the rheological characterisation of the material. Figure 3a shows the microstructure of the material before shearing within the shear cell. A dense array of oil droplets can be identified. When the material was submitted to shear rates below of order 1 s^{-1} all of the droplets were observed to move together and with the same velocity as the moving bottom glass disc. The emulsion under these conditions was slipping at an interface between the fluid and the top stationary glass disc. As the applied shear was increased above 1 s^{-1}, relative movement becomes

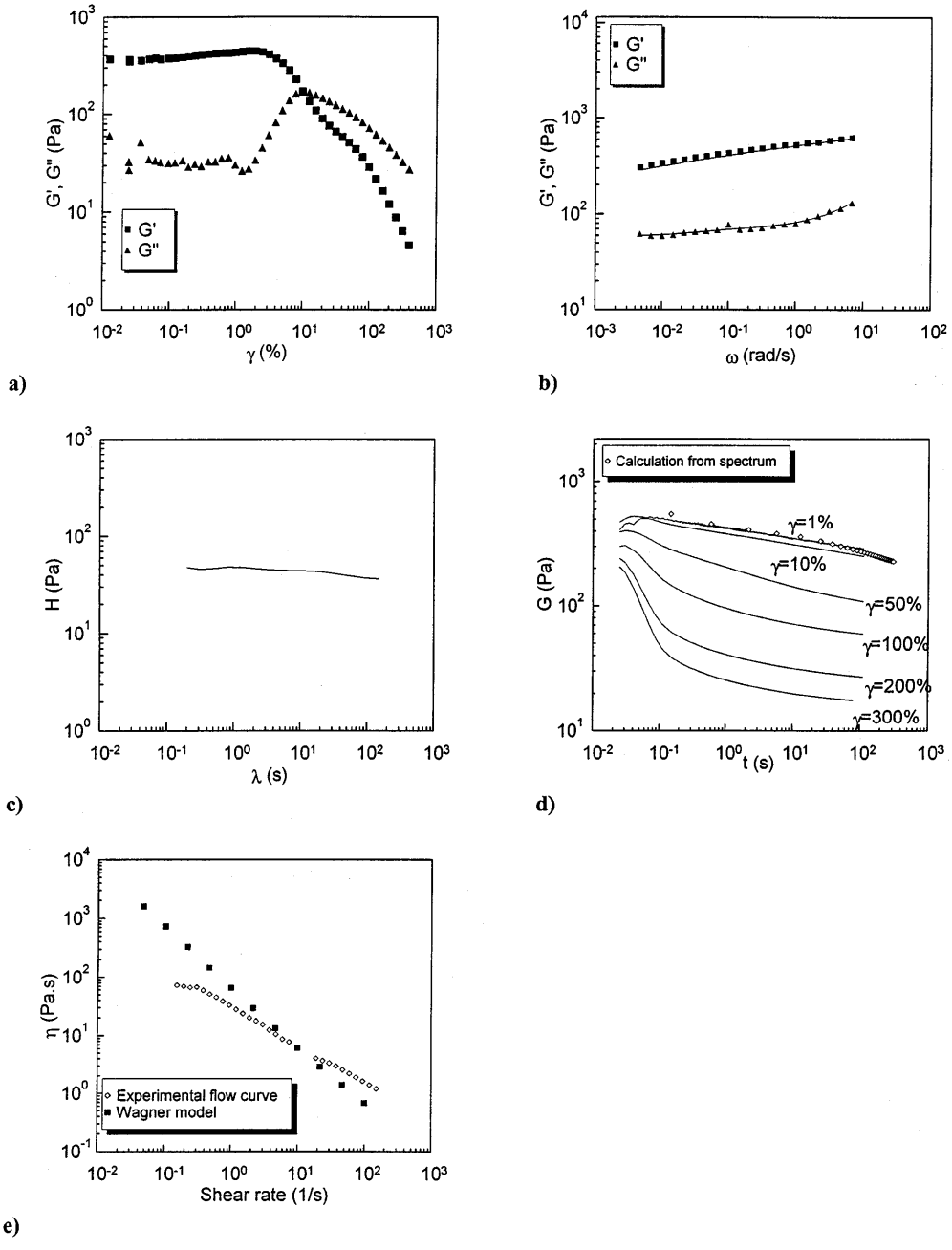

Fig. 2 Rheological characterisation of a commercial mayonnaise **a** strain sweep (ω = 6.28 rad/s); **b** frequency sweep (γ = 0.4%) with continuous linear relaxation spectrum fit; **c** continuous linear relaxation spectrum; **d** linear and non-linear relaxation modulus with continuous linear relaxation spectrum fit; **e** experimental and model prediction of steady-state flow curve

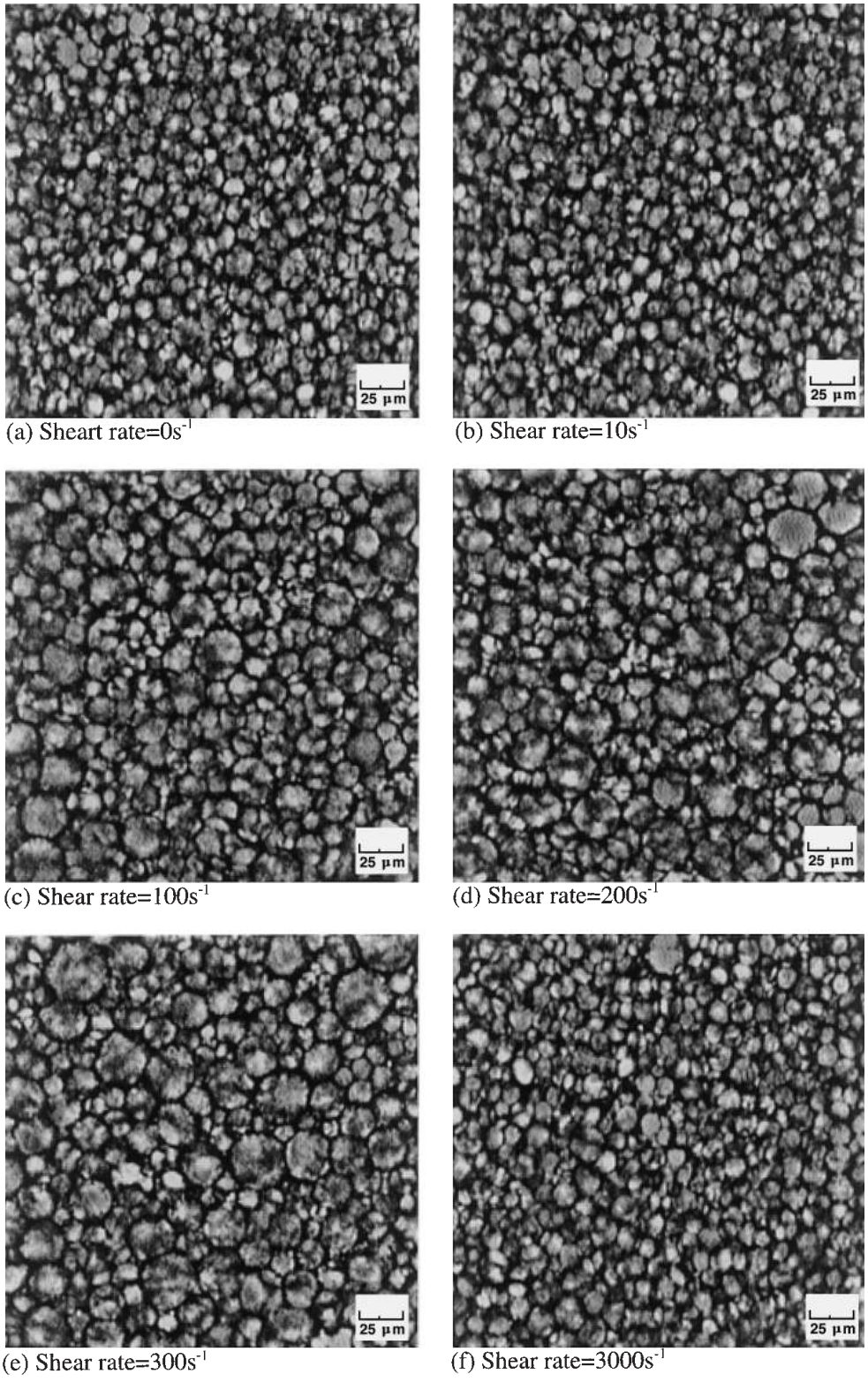

Fig. 3 Optical micrographs of a commercial mayonnaise: **a** 0 s^{-1}; **b** 10 s^{-1}; **c** 100 s^{-1}; **d** 200 s^{-1}; **e** 300 s^{-1}; **f** 3000 s^{-1}. Samples thickness of order 50 μm. Photographs taken immediately after shear

apparent between adjacent droplets and the material appeared to move as a continuum with little or no relative slip at the top and bottom glass interface. At shear rates higher than 10 s^{-1}, the size of the oil droplets was clearly seen to increase, due to coalescence of droplets, as shown in Fig. 3c–e for shear rates comprised

between 100 and 300 s^{-1}. At much higher shear rates ($>1000\ s^{-1}$) the droplets were disrupted to a size approaching that of the unsheared sample. The photomicrographs of the mayonnaise microstructure were of sufficient quality to facilitate in situ size measurement of the droplet size distribution (DSD) of the sample under different shearing conditions by using image analysis techniques.The corresponding DSD are shown in Fig. 4. The similarity of the size distributions at 10 and 3000 s^{-1} and the much larger size of emulsion droplets at 300 s^{-1} are apparent.

Pea protein-stabilised emulsion

The rheological data of the pea protein-stabilised emulsion are shown in Fig. 5. The rheological behaviour is very similar to that shown by the commercial mayonnaise previously studied. The strain sweep of Fig. 5a shows that again the linear region is limited to quite small strains of less than 1%. A frequency sweep performed at a strain within the linear region (0.4%) shows a frequency dependence similar to that of the commercial mayonnaise, a predominantly elastic behaviour with G′ greater than G″ for the entire frequency range. Figure 5b shows the frequency sweep data fitted with a continuous spectrum of relaxation times, which gives a good recalculation of the dynamic viscoelasticity functions over the whole frequency range studied. Figure 5c shows the continuous spectrum of relaxation times for this emulsion. A predominant "plateau" region in the time domain tested, with almost unvariant stiffness values, is apparent. The step strain data of Fig. 5(d) showed that the pea protein-stabilised emulsion had a more pronounced non-linear behaviour compared to the commercial mayonnaise. Thus, a relatively small increase in the applied strain from 1% to 10% results in a marked decrease in the relaxation modulus, which is reflected in a higher value of the Wagner damping factor ($h = 2.2$). The prediction of the steady shear behaviour using a factored constitutive equation with Wagner damping function is given in Fig. 5e. The model prediction of the steady-state flow response is similar to that for the commercial mayonnaise at low shear rates, with overestimation of the apparent viscosity. In contrast, the fitting is fairly good for shear rates comprised between 4 and 100 s^{-1}.

The optical observations for the pea protein-stabilised emulsion are shown in Fig. 6 for a series of different shearing conditions. Figure 6a demonstrates that the mean droplet diameter of this emulsion before shearing was significantly lower than that of the commercial mayonnaise previously studied. At low shear rates ($<4\ s^{-1}$) the behaviour was identical to that of the commercial mayonnaise; that is, the sample was seen to undergo slip between the quartz discs of the shear cell. As the shear rate was increased above that critical shear rate, relative movement between oil droplets visibly increased. In contrast to the commercial mayonnaise, an increase in shear rate up to 300 s^{-1} did not modify the droplet size distribution of the emulsion, as shown in Fig. 6c–e. At much higher shear rates ($>1000\ s^{-1}$) the droplets were disrupted by the shear stress to a size lower than that of the unsheared sample, as seen in Fig. 6f.

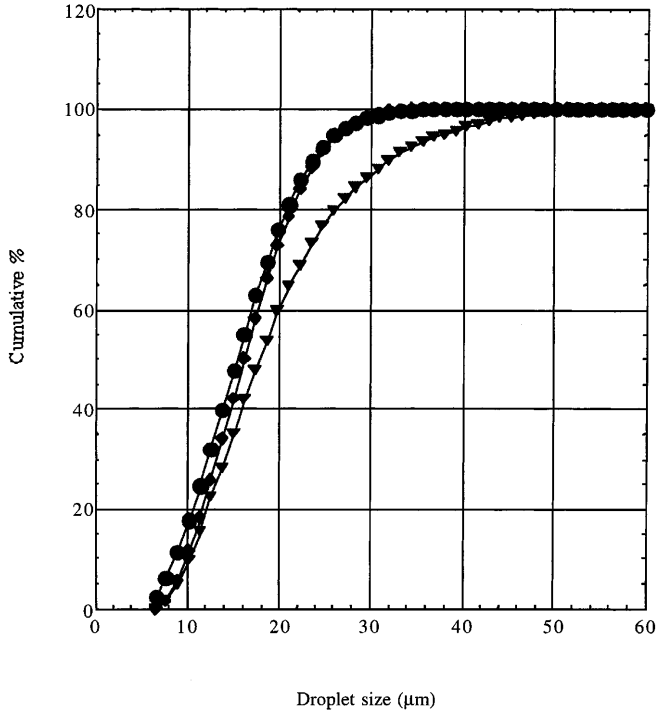

Fig. 4 Droplet size distribution curves, for a commercial mayonnaise, as a function of the shear rate applied on the sample

PEG/non-ionic-surfactant-stabilised emulsion

Rheological data for this emulsion, which is clearly different to those previously shown, because it is stabilised by a low-molecular-weight emulsifier and consequently the nature of the interdroplet interactions is more typical of a "particle gel" (Dickinson and Hong 1995) are shown in Fig. 7. The experimental results obtained show some significant differences from the previous two emulsions. Firstly, the linear region is very much smaller than before and also clear deviations from linearity are shown in Fig. 7a at strain levels exceeding 0.3%. However, the frequency dependence of its dynamic linear viscoelasticity functions (Fig. 7b) is similar to that of a highly flocculated emulsion, showing a clear "plateau" region in G′ and a tendency to a minimum in G″, which is not reached due to the limitation in the reliability of the high frequency values because of its

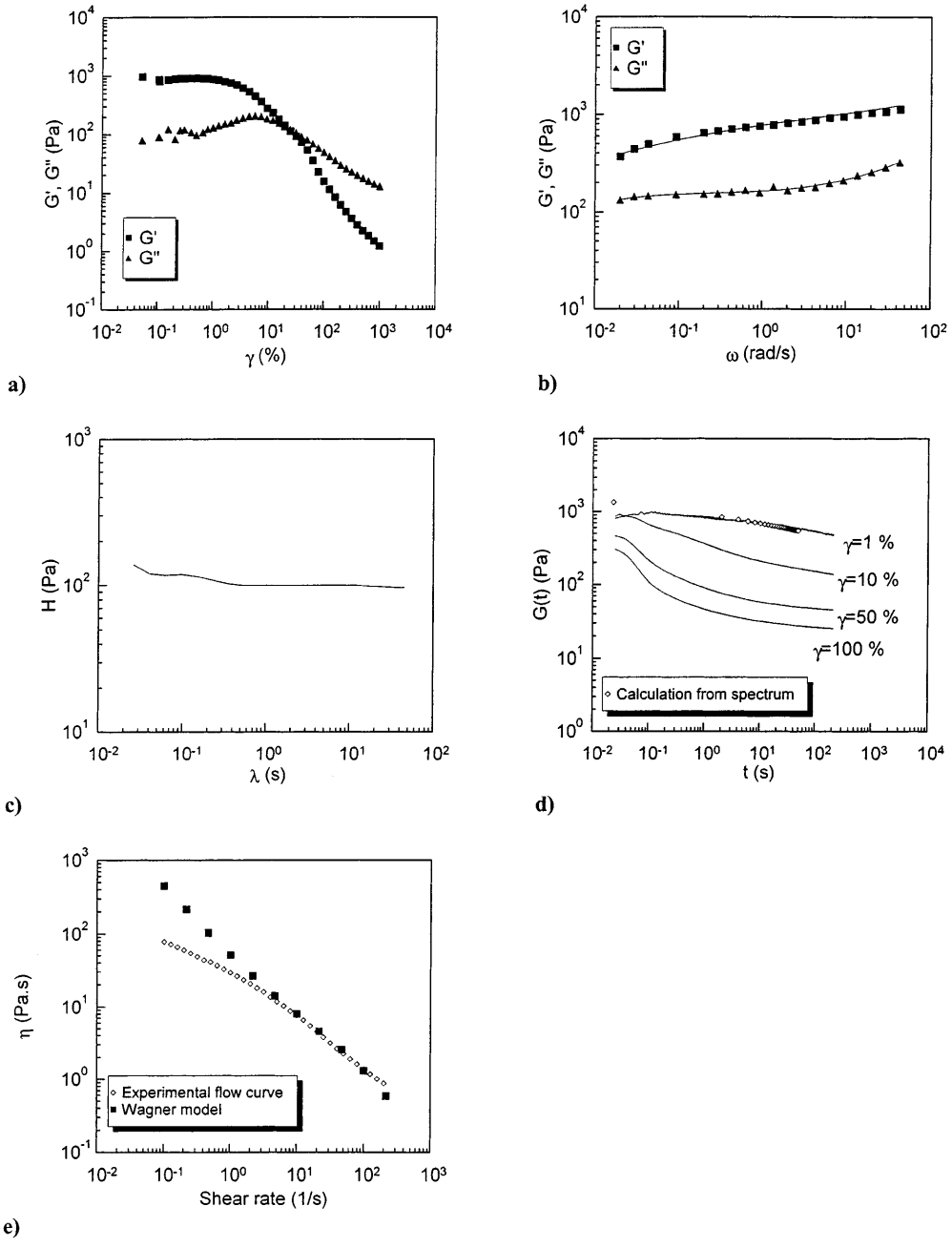

Fig. 5 Rheological characterisation of a vegetable protein-stabilised emulsion: **a** strain sweep (ω = 6.28 rad/s); **b** frequency sweep (γ = 0.4%) with continuous linear relaxation spectrum fit; **c** continuous linear relaxation spectrum; **d** linear and non-linear relaxation modulus with continuous linear relaxation spectrum fit; **e** experimental and model predication of steady-state flow curve

extremely narrow linear viscoelasticity range. The continuous relaxation spectrum (Fig. 7c), shows now two different regions: a transient region for the lowest relaxation times and a "plateau" region, with a significant positive slope, once again typical of highly flocculated emulsions. The step strain response is shown in Fig. 7d and it is reassuring to note that the relaxation modulus predicted from the G′, G″ data is in good agreement with the small strain, experimental step strain data. The large strain data in Fig. 7d give a damping factor of k = 0.62. The prediction of the steady-state shear data using the Wagner model is given in Fig. 7e. At shear rates below 2 s^{-1} the fit between model and experimental data is poor. This poor match may again be interpreted as a consequence of the development of wall-slip phenomena during steady shear. At shear rates between 2 and 100 s^{-1} the continuous spectrum data fit can match the steady-state flow behaviour fairly well. However, for shear rates larger than 100 s^{-1} the model fit slightly deviates from the experimental data, in a similar way to the lack of agreement found in this region of the flow curve for the pea protein-stabilised emulsion.

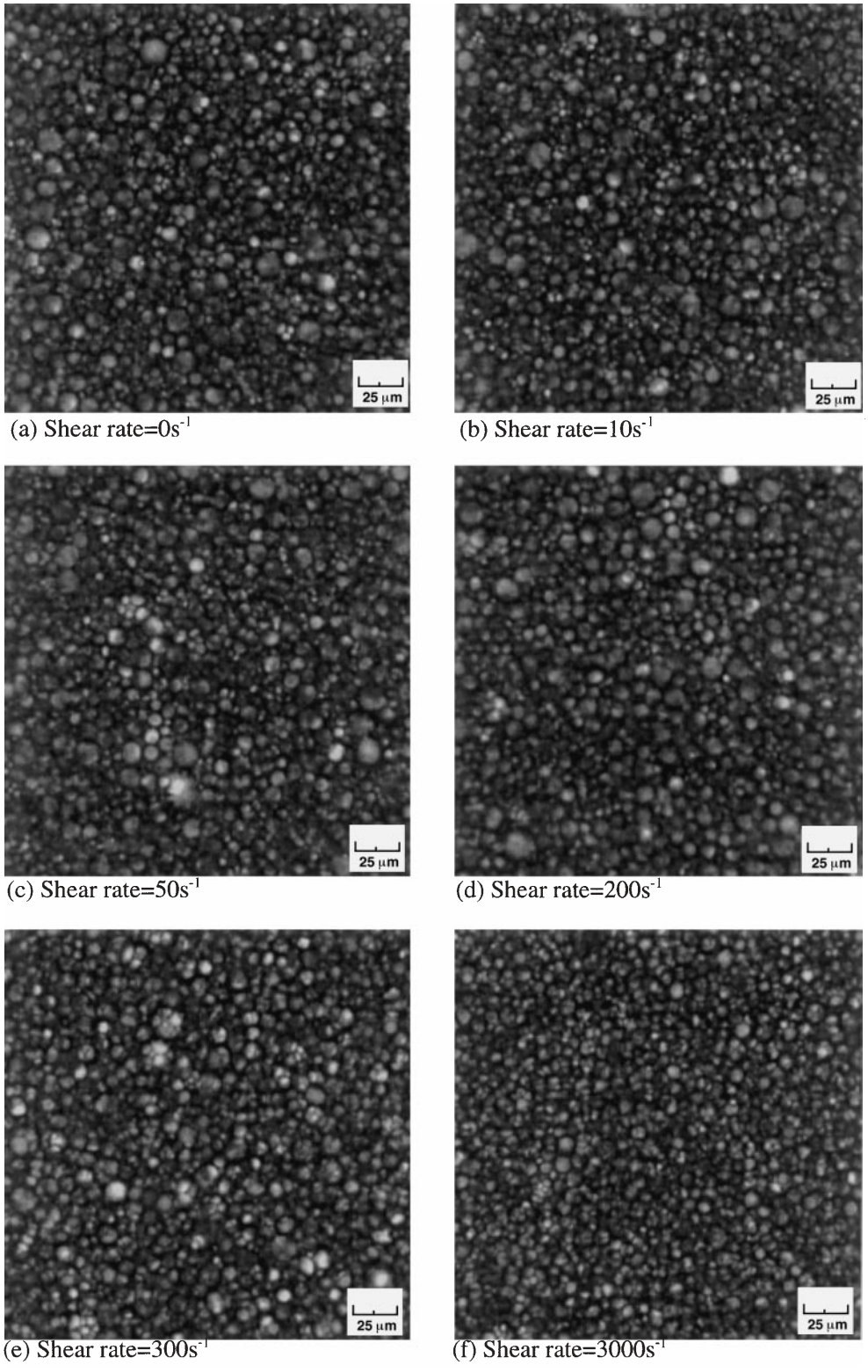

Fig. 6 Optical micrographs of a vegetable protein-stabilised emulsion: **a** 0 s^{-1}; **b** 10 s^{-1}; **c** 50 s^{-1}; **d** 200 s^{-1}; **e** 300 s^{-1}; **f** 3000 s^{-1}. Sample thickness of order 50 μm. Photographs taken immediately after shear

This deviation can partly be explained by the truncation of the relaxation spectrum in the short time scale. If this is extended by extrapolating the G′ and G″ data given in Fig. 7b, a very much better fit can be obtained in the high shear rate region without significantly influencing the results at lower shear rates.

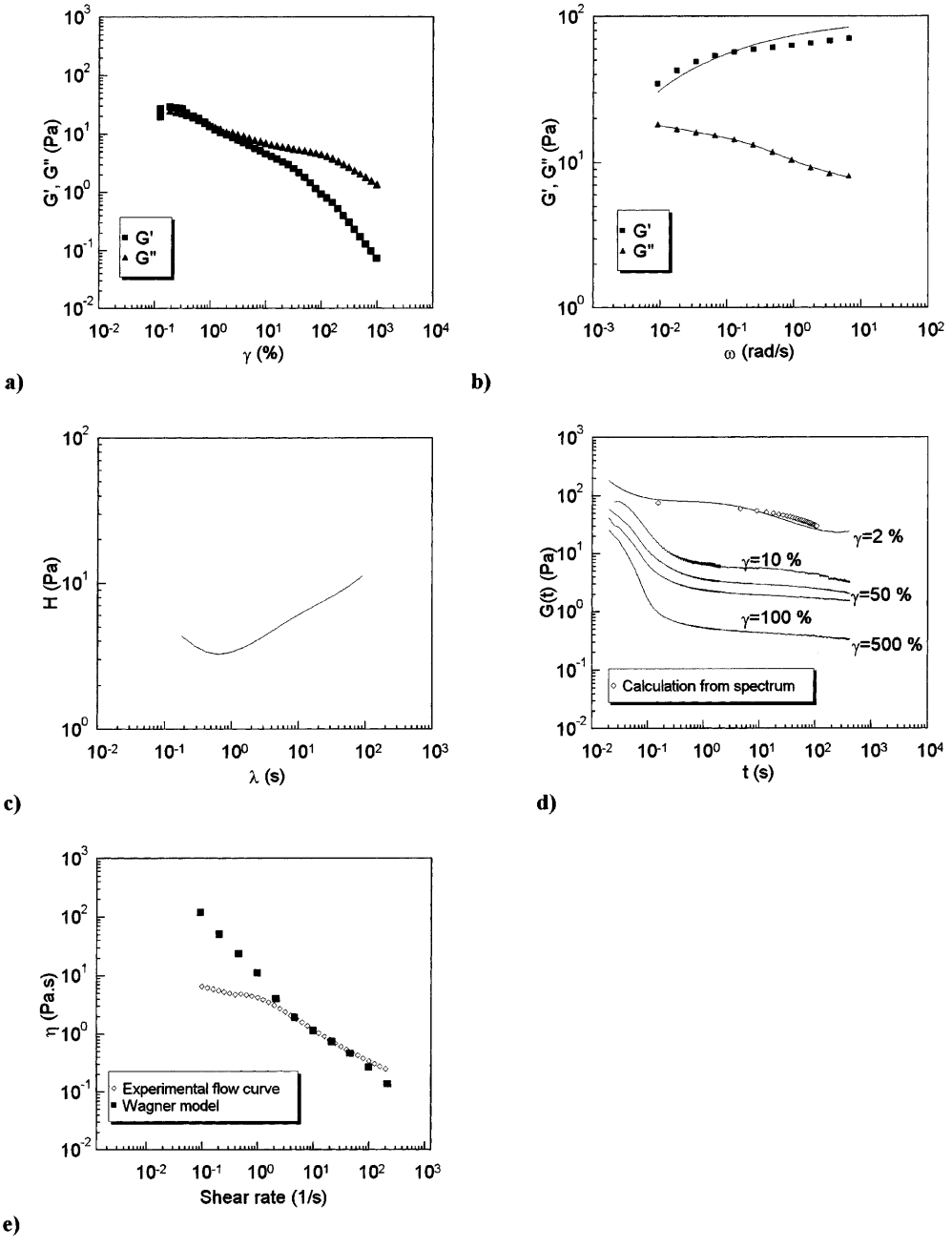

Fig. 7 Rheological characterisation of a polyoxyethylene glycol nonylphenyl ether-stabilised emulsion: **a** strain sweep (ω = 6.28 rad/s) **b** frequency sweep (γ = 0.3%) with continuous linear relaxation spectrum fit; **c** Continuous linear relaxation spectrum; **d** linear and non-linear relaxation modulus with continuous linear relaxation spectrum fit; **e** experimental and model prediction of steady-state flow curve

Microstructure observations of the emulsion revealed a much finer dispersion of oil droplets compared to the pea protein-stabilised and commercial mayonnaise emulsions. Thus, the oil droplets are so small that they appear as a continuous background. The average droplet size is less than 1 μm; however, some larger droplets (>10 μm) were also present. Application of shear rates lower than 100 s^{-1} caused no visible changes in the emulsion microstructure; however, at shear rates comprised between 100 and 300 s^{-1} the largest droplets were seen to align into chains along the shear direction. The chaining behaviour seen in this system has also been observed in viscoelastic polymer fluids (Michele et al. 1977). At very high shear rates (1000 s^{-1}) the droplet chains were disrupted and the emulsion microstructure looked very similar to that of the unsheared sample.

Sucrose ester-stabilised emulsion

The rheology of the sucrose ester-stabilised emulsion showed further clear differences, mainly due to the fact

that this emulsion does not possess a linear viscoelasticity region even at strains as low as 0.1%, as seen in Fig. 8a. The frequency sweeps shown in Fig. 8b therefore have to be treated with caution. In fact, the evolution is completely different to that found with other sucrose ester-stabilised emulsions, which show a clear "plateau" region. Consequently, strains outside the linear viscoelasticity range modify the interdroplet interactions responsible for this region, and also favour the appearance of the terminal region in the frequency range studied. The non-linear step strain data (Fig. 8c) follow a similar pattern to those shown by other emulsions, but the steady-state flow results given in Fig. 8d show a peculiar response. Thus, the experimental data appear to follow two distinct regions. For shear rates lower than 10 s^{-1} the material behaves as Newtonian. Above this shear rate significant shear thinning is observed.

Experimental observations of the sucrose ester-stabilised emulsion microstructure in the optical shear cell confirmed the peculiarities raised by the rheological characterisation. At rest, the sucrose ester-stabilised emulsion was seen to be a relatively uniform dispersion of oil droplets, visible as light circles in the photomicrograph of Fig. 9a. The sucrose ester was also visible as dark regions between the oil droplets. It is thought that the sucrose ester formed a continuous matrix interdispersed with oil droplets. Application of small steady shear rate of 10–50 s^{-1} led to coalescence of the oil droplets and a disruption of the gel-like sucrose ester matrix. Figure 9b and 9c clearly shows the increased size of the oil droplets and the separation of the sucrose ester (black regions) into discrete clusters within the microstructure of the emulsion. Slippage of the sample between the quartz discs of the shear cell was also apparent, but in addition to this, movement of "microdomains" within the emulsion matrix was also observed. The sample was seen to fracture into irregular domains several hundred of micrometres across which moved relative to one another as a result of the applied shear stress. These microdomains were similar in appearance to the grain boundaries in crystalline materials, with emulsion droplets inside the domains showing no relative movement. At intermediate shear rates of 20–300 s^{-1} the emulsion became much more fluid-like with increased mobility and relative motion of the oil droplets within the sample. At shear rates of 200–300 s^{-1} chaining of the oil droplets was apparent. As was seen with the PEG non-ionic surfactant-stabilised emulsion, the oil droplets formed chains consisting of several droplets aligned along the direction of the applied shear. At high shear rates (600 s^{-1}) droplet alignment disappeared and the larger oil droplets were disrupted to yield a more uniform emulsion similar to the original unsheared material. Shearing of the sample at 1000 s^{-1} for a period of approximately 5 min resulted in the formation of large gel-like particles of the sucrose ester. Once the emulsion reached this condition it was not possible to return to the original state without the application of heat to melt the sucrose ester aggregates.

Discussion and conclusions

In this paper the rheology and microstructure of four different oil-in-water emulsions has been experimentally surveyed and the fit of the rheological data to one class of constitutive equation has been attempted.

At small strains all of the emulsions had a significant viscoelastic response and two systems had a clear linear viscoelastic region. The linear viscoelastic frequency response was fitted to a continuous relaxation spectrum. From the data presented in this paper it is clear that three of the emulsions tested possessed a broad relaxation "plateau" within the time domain examined (10^{-1}–10^{2} s); this observation is consistent with the findings of others where a wide "plateau region" has been reported for the viscoelastic spectrum (Gallegos et al. 1992b).

Good self-consistency was observed between the linear relaxation modulus generated from G' and G'' data and that obtained from small strain, step strain data. For larger strain, step strain data exhibited the classic hallmark of factorability for strain, characterised by a reduction in the relaxation modulus without a major change in the slope of the stress decay. This is a key point and supports the justification for fitting the experimental data to a Wagner-type equation. The strain softening of the materials was characterised using a Wagner damping factor k, with values for k ranging from 0.6 to 2.2. This compares with a typical value of 0.3 for a polymer melt and confirms the experimental observation that emulsion viscoelasticity is delicate, and limited to smaller strain deformations than most polymer systems.

The model predictions for steady shear were compared with experimental data and the quality of the observed match varied depending on both shear rate regime and material composition. A key feature of the steady shear data observed for all samples is that the predicted low shear data are greater than that experimentally observed. This is consistent with the observation of slip seen at low shear rates using the optical shear cell. This observation of slip is also consistent with the conclusions of others (Barnes 1995; Franco et al. 1998) and obviously has important consequences in terms of interpretation of any steady shear data from emulsion systems. Thus, low-shear-rate wall-slip effects appear to be a generalised problem in emulsion rheology. It may also influence the width of the linear viscoelasticity region, as previously stated by other authors (Diogo 1995). This may explain why no linear viscoelasticity region has been found in the sucrose stearate-stabilised emulsion. In fact, this system shows the largest wall-slip

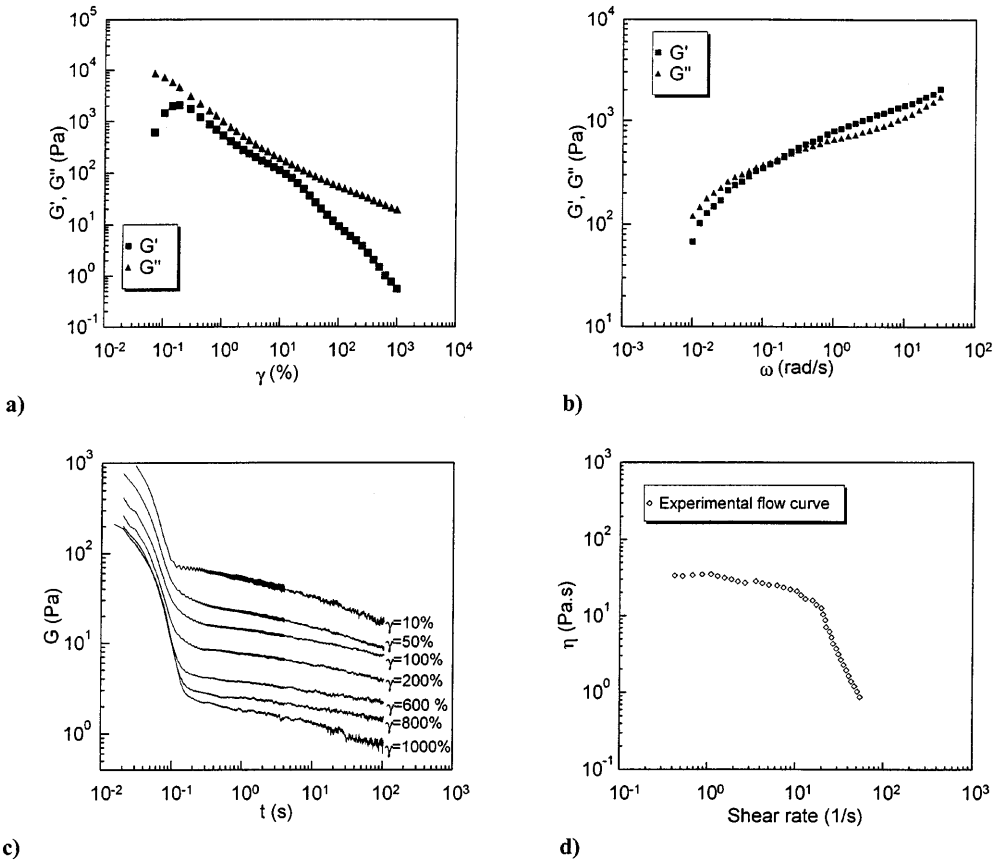

Fig. 8 Rheological characterisation of a sucrose ester-stabilised emulsion **a** strain sweep (ω = 6.28 rad/s); **b** frequency sweep (γ = 0.3%); **c** non-linear relaxation modulus; **d** experimental steady-state flow curve

effects, with a "pseudo"-Newtonian region at shear rates comprised between 0.1 and 10 s^{-1}.

An additional striking feature of the steady shear rheological data can be seen if the steady shear predictions for the continuous spectrum model are examined for all the emulsions. Over the shear rate range of order 10^{-1}–10^{2} s^{-1}, the steady shear flow stress is almost constant for each sample. The value of the flow stress varies for each emulsion and ranges from 10 Pa for the non-ionic surfactant emulsion to 100 Pa for the sucrose ester emulsion. The origin of the stress at different shear rates can be correlated as originating from the components of the relaxation spectrum where λ is of order $1/\dot{\gamma}$. This may have important consequences in interpreting the mechanism associated with stress generation in emulsions.

The optical microstructure observation made during shear revealed a number of additional features. In certain systems such as the vegetable protein-stabilised emulsion little or no change in droplet size distribution (DSD) was observed as a consequence of shear for much of the shear rate examined and in this case reasonable agreement was found between model steady shear data and experiment. For the case of mayonnaise, however, droplet coalescence was observed at intermediate shear rates (probably due to a wrong storage, which induced lower viscoelastic characteristics than expected) and, in this region of the flow curve, a relatively poor fit between the model and experiment was found. These observations suggest that when the change in microstructure with shear is mainly related to a deflocculation process, a factorable constitutive equation can be used; if, however, the DSD does change, this assumption cannot necessarily be made. Consequently, if the wall-slip phenomena and DSD changes are avoided, the Wagner constitutive equation should predict the steady-state flow behaviour of emulsions in a very wide range of shear rate. This fact is confirmed in Fig. 10, where the experimental steady-state flow curve of the vegetable protein stabilised emulsion, obtained in a controlled stress rheometer using a serrated plate-plate geometry, is matched with that predicted from the Wagner model, in a shear rate range comprised between 10^{-6} and 10^{-3} s^{-1}.

Concentrated emulsions appear to fall into a general rheological class of behaviour characterised by a "plateau" relaxation spectrum and a factorable strain softening damping factor. Although concentrated emul-

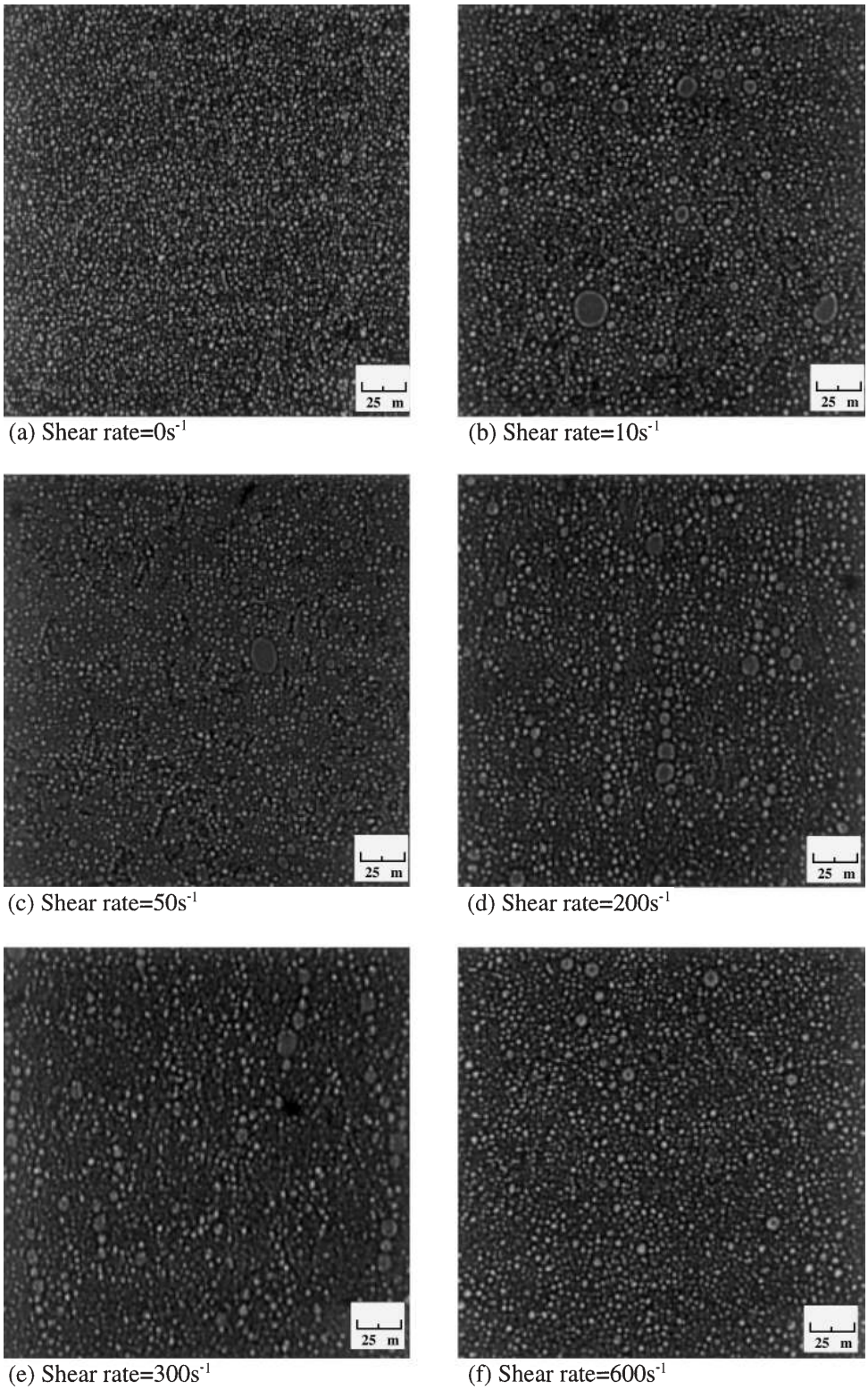

Fig. 9 Optical micrographs of a sucrose ester-stabilised emulsion: **a** 0 s^{-1}; **b** 10 s^{-1}; **c** 50 s^{-1}; **d** 200 s^{-1}; **e** 300 s^{-1}; **f** 600 s^{-1}. Samples thickness of order 50 μm. Photographs taken immediately after shear

sions have high viscoelasticity at small strain deformations, they also strain soften to give an essentially viscous fluid at large strain deformations and in steady shear. The Wagner integral equation appears to do a reasonable job in characterising the steady-state flow behaviour of concentrated emulsions, although it is

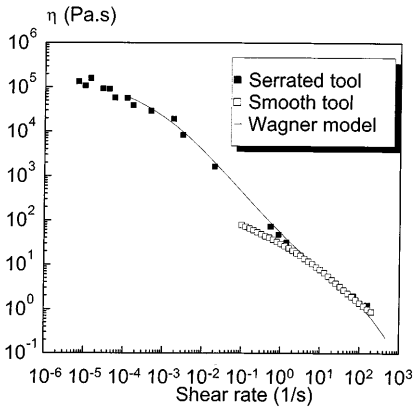

Fig. 10 Experimental and model prediction of steady-state flow curve, for vegetable protein-stabilised emulsion, using **a** smooth plate-and-plate geometry in a controlled-strain rheometer, and **b** profiled plate-and-plate geometry in a controlled-stress rheometer

almost certainly not a unique constitutive equation that can describe the observed behaviour. Wall slip, changes in droplet size distribution and microdomain flow are all factors that may cause deviation from the base emulsion behaviour.

This paper has provided a microscopic and phenomenological description of the rheology of concentrated oil-in-water emulsions. It has not proved possible to link completely the observed microstructure changes with the rheological behaviour. However, the observed low shear slip does, for example, correlate with the overprediction of the model steady shear stress, in relation to the experimental values, for low shear rates. In addition, the small change in observed droplet size for the shear range tested also supports the view that the material can be described using a factored memory function. What is now required is a greater depth in understanding the mechanism of viscoelasticity for concentrated emulsions, task that has been already addressed by several authors [see, for example, Princen (1983) and Kraynik et al. (1991)].

Acknowledgements We would like to thank Acciones Integradas, a British Council/Spanish joint collaborative fund for providing some financial support for this work. C. Bower would also like to thank the Cambridge Colloid Technology Programme for financial assistance.

References

Barnes HA (1994) Rheology off emulsions - a review. Colloids Surf A 91:89–95

Barnes HA (1995) A review of the slip (wall depletion) of polymer solutions, emulsions and particle suspensions in viscometers: its cause, character and cure. J Non-Newtonian Fluid Mech 56:221–251

Bower C, Mackley MR, Smeulders BAS, Barker D, Hayes J (1997) The rheology, processing and microstructure of complex fluids. In: Ottewill RH Colloid dispersions. Rennie AR (eds) Kluwer, Dordrecht. pp 279–289

Dickinson E, Hong ST (1995) Influence of water-soluble nonionic emulsifier on the rheology of heat-set protein-stabilized emulsion gels. J Agric Food Chem 43:2560–2566

Diogo (1995) Rheology of liquid foams under shear: transient shear, steady shear and exponential (strong) shear flows. Cah Rheol 14:231–240

Franco JM, Guerrero A, Gallegos C (1995) Rheology and processing of salad dressing emulsions. Rheol Acta 34:513–524

Franco JM, Berjano M, Gallegos C (1997) Linear viscoelasticity of salad dressing emulsions. J Agric Food Chem 45:713–719

Franco JM, Gallegos C, Barnes HA (1998) On slip effects in steady-state flow measurements on o/w food emulsions. J Food Eng 36:89–102

Gallegos C, Franco JM (1995) Linear and non-linear viscoelasticity food emulsions containing a mixture of two emulsifiers. Cah Rheol 14:107–116

Gallegos C, Berjano M, Guerrero A, Muñoz J, Flores V (1992a) Transient flow of mayonnaise described by a nonlinear viscoelasticity model. J Texture Stud 23:153–168

Gallegos C, Berjano M, Choplin L (1992b) Linear viscoelastic behavior of commercial and model mayonnaise. J Rheol 36:465–478

Guerrero A, Partal P, Berjano M, Gallegos C (1996) Linear viscoelasticity of o/w sucrose palmitate emulsions. Prog Colloid Ploym Sci 100:246–251

Kraynik AM, Reinelt DA, Princen HM (1991) The nonlinear elastic behavior of polydisperse hexagonal foams and concentrated emulsions. J Rheol 35:1235–1253

Larson RG (1988) Constitutive equations for polymer melts and solutions. Butterworth, Boston

Mackley MR, Marshall RTJ, Smeulders JBAF, Zhao FD (1994) The rheological characterization of polymeric and colloidal fluids. Chem Eng Sci 49:2551–2565

Madiedo JM, Gallegos C (1997) Rheological characterization of oil-in-water emulsions by means of relaxation and retardation spectra. Recent Res Dev Oil Chem 1:79–90

Madiedo JM, Muñoz J, Gallegos C (1996) Calculation of relaxation and retardation spectra using the Tikhonov regularization method: application to emulsions. In: Signer DA, Advani SG (eds) Rheology and fluid mechanics of nonlinear materials AMD, vol 217. ASME, New York, pp 151–159

Michele J, Patzold R, Donis R (1977) Aligment and aggregation effects in suspensions of spheres in non-Newtonian media. Rheol Acta 16:317–321

Pal R, (1992) Rheology of polymer-thickened emulsions. J Rheol 36:1245–1259

Pal R, Rhodes E (1989) Viscosity/concentration relationships for emulsions. J Rheol 33:1021–1045

Partal P, Guerrero A, Berjano M, Muñoz J, Gallegos C (1994) Flow behavior and stability of oil-in-water emulsions stabilized by a sucrose palmitate. J Texture Stud 25:331–348

Princen HM (1983) Rheology of foams and highly concentrated emulsions. J Colloid Interface Sci 91:160–175

SosKey PR, Winter HH (1984) Large step shear strain experiments with parallel-

disk rotational rheometers. J Rheol 28:625–645
Tadros TF (1993) Fundamental principles of emulsion rheology and their applications. First World Congress on Emulsions, vol 4., pp 237—265
Wagner MH (1976) Analysis of time-dependent non-linear stress growth data for shear and elongational flow of a low-density branched polyethylene melt. Rheol Acta 15:136—142
Wagner MH, Schaeffer J (1993) Rubbers and polymer melts: Universal aspects of nonlinear stress-strain relations. J Rheol 37:643—661